Structural analysis of Fe/Cr superlattices and their components

1998 J. Phys.: Condens. Matter 10 61

(http://iopscience.iop.org/0953-8984/10/1/007)

J. Phys.: Condens. Matter **10** (1998) 61–66. Printed in the UK PII: S0953-8984(98)86074-8

Structural analysis of Fe/Cr superlattices and their components

R Schad†‡‖, D Bahr§¶, J Falta§, P Beliën†+ and Y Bruynseraede†

† Laboratorium voor Vaste-Stoffysika en Magnetisme, KU Leuven, 3001 Leuven, Belgium
‡ Research Institute for Materials, KU Nijmegen, 6525 ED Nijmegen, The Netherlands
§ Hamburger Synchrotronstrahlungslabor at DESY, Notkestrasse 85, 22607 Hamburg, Germany

Received 16 July 1997

Abstract. Structural analysis of metallic superlattices is essential for understanding their interesting transport properties like the giant magnetoresistance (GMR) effect. We present a detailed analysis of the [Fe (4.8 Å)/Cr (13 Å)]$_{50}$ superlattice which shows a record GMR value. The analysis is done by simulating its x-ray diffraction spectrum measured with a synchrotron x-ray source. The ingredients for this simulation are obtained from simulations of x-ray diffraction spectra of single Fe and Cr films. This way we reduce the number of free parameters resulting in reliable values for the interfaces roughness. We also show that x-ray diffraction spectra of systems with low contrast in electron density can be quantitatively analysed.

1. Introduction

Metallic superlattices often have novel properties [1, 2] like the giant magnetoresistance (GMR) observed in magnetic multilayers. This effect is believed to be caused by spin-dependent electron scattering at the interface imperfections [3–7]. Therefore, structural analysis of these multilayers is necessary to understand the electron transport properties. X-ray diffraction (XRD) [8] is one of the most powerful structure analysis techniques for two reasons. First, it is a non-destructive technique with a high penetration depth allowing application after completion of the sample growth. Thus XRD probes the whole superlattice as it is also seen by the electrons in the transport measurements. Second, the x-ray wavelength used is similar to the Fermi wavelength of usual metals, thus probing the sample at the same length scale as the electrons do. The analysis of a multilayer structure is done by simulation of its x-ray diffraction spectrum where a large number of input parameters enter [9–12]. However, for the important parameters (such as the interface roughness σ) reliable and 'robust' values have to be obtained. This requires that other parameters, for instance the ones describing the properties of the top oxide layer, are determined in independent experiments.

We will present a detailed structure analysis of epitaxial Fe and Cr films and an [Fe (4.8 Å)/Cr (13 Å)]$_{50}$ superlattice showing 220% magnetoresistance [13]. The

‖ Corresponding author: Dr Rainer Schad, Research Institute for Materials, Katholieke Universiteit Nijmegen, Toernooiveld 1, NL 6525 ED Nijmegen, The Netherlands. Tel: +31 (0)24 3653094. Fax: +31 (0)24 3652190. E-mail address: schad@sci.kun.nl
¶ Present address: AXS, Postfach, D-76181 Karlsruhe, Germany.
+ Present address: Philips Optical Storage, Kempische Steenweg 293, 3500 Hasselt, Belgium.

0953-8984/98/010061+06$19.50

quantitative agreement between measurement and simulation also proves that XRD spectra of systems with low contrast in the electron density can be analysed quantitatively.

2. Experimental details

The superlattices were prepared in a Riber MBE deposition system (2×10^{-11} mbar base pressure) equipped with electron beam evaporators which were rate stabilized to within 1% by a home made feedback control system [14] using Balzers quadrupole mass spectrometers (QMS). Additionally, integration of the QMS signal was used to automatically control the shutters of the individual evaporation sources. Calibration of the QMS signals was done by comparison with the evaporation rates measured with a quartz crystal thickness controller and measuring thicknesses of test samples by small-angle (SA) XRD and profilometry. The samples were grown with the substrate holder rotated at 60 rpm ensuring a homogeneous layer thickness. The Fe and Cr layers (starting material of 99.996% purity) were evaporated in a pressure of 4×10^{-10} mbar at a rate of 1 Å s^{-1} on single-crystalline MgO(001) substrates (typically 5×10 mm^2). The surface roughness of the MgO(001) substrates was evaluated *ex situ* by atomic force microscopy (AFM). Typically the MgO surfaces have an rms roughness of 4 Å measured over 1 μm^2 areas. After rinsing in isopropyl alcohol and drying in a dry N_2 flow, the substrate was annealed at 600 °C in UHV for 15 minutes. The data presented here are for single Fe and Cr layers (about 300 Å thick) and an [Fe (4.8 Å/Cr (13 Å)]$_{50}$ superlattice grown on a 50 Å Cr buffer. The substrate temperature during growth was 50 °C.

Structural information about the superlattices was obtained from SA XRD measurements using a synchrotron radiation source (ROEMO 1 at HASYLAB) with wavelength 1.078 Å. The XRD spectra were measured in symmetric θ–2θ geometry.

3. Results and discussion

First we will discuss the properties of single Fe and Cr layers grown on MgO(001) because their structural parameters will enter the simulation of the XRD spectrum of the superlattice. The growth is epitaxial as seen by reflection high-energy electron diffraction (RHEED) *in situ* and off-axis XRD at high angle *ex situ* obeying the epitaxial relationship Fe(Cr) (001)[100] ∥ MgO (001)[110]. This means that bcc Fe or Cr layers grow with an in-plane 45° rotation with respect to the axes of the fcc MgO substrate leading to an in-plane lattice misfit of only 3.5%. Since the samples are not covered by a protection layer the surface is expected to oxidize. The composition and thickness of this oxide layer are in principle unknown and also might change with time. However, inspection by eye shows that such Fe and Cr films look metallic after years of storage under ambient conditions. XRD spectra taken respectively directly after growth or months later are identical. This indicates that the top layers of the metal oxidize rapidly after exposure to air [15] forming an oxide of defined, constant thickness which protects the rest of the metal film from further oxidation. In particular, Cr can be employed advantageously as a protection layer for oxidizable structures even when the Cr film does not grow epitaxially. The properties of the oxide and the metallic layer underneath are obtained by evaluating the XRD spectra shown in figure 1 for a single Fe and single Cr film. The oxcillations with different periods stem from interference of x-ray beams reflected at the different interfaces. The interference of the beams reflected at the sample surface and at the film–substrate interface produce the fast oscillations (called Kiessig fringes), so are related to the total film thickness, whereas the long-wavelength modulation is caused by the thin oxide layer. The quantitative simulation

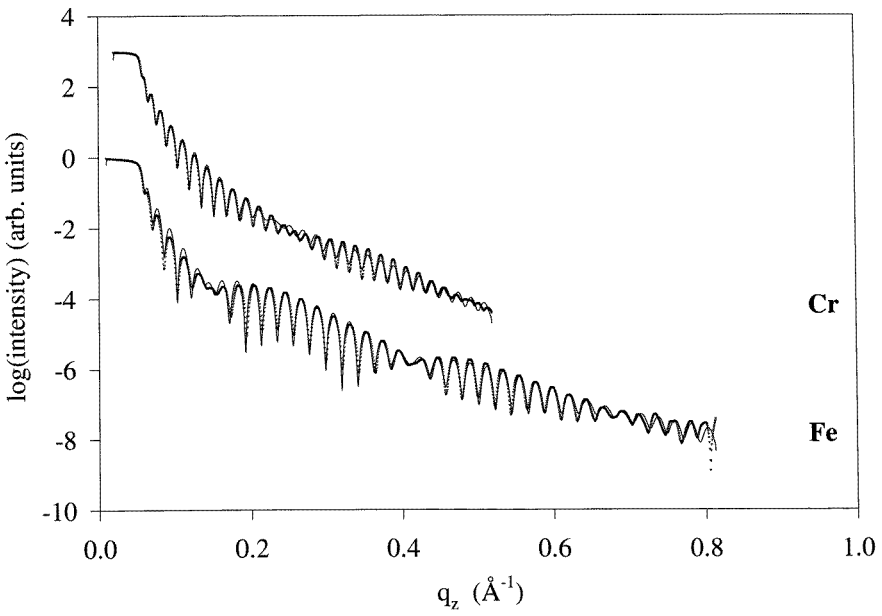

Figure 1. Specular XRD intensity as a function of the vertical scattering vector q_z. The measured spectra (data points) and simulations (thin lines) of an Fe and a Cr film are shown. The parameters of the simulations are summarized in table 1. The Fe and Cr spectra are offset for clarity.

of the spectra (figure 1) reveals all important parameters as summarized in table 1. Because of the epitaxial growth with about 3.5% lattice mismatch between film and substrate one would expect the films to be strained. Indeed, we found a slight tetragonal distortion in form of a slight expansion of the lattice parameter in the film plane and a 0.5% contraction in the perpendicular direction using high-angle XRD. However, for SA XRD the atomic structure is not directly relevant and only enters via the electron density of the layers. All spectra presented could be fitted with Fe and Cr bulk electron density indicating an unchanged volume of the unit cell, i.e. a compensation of in-plane expansion and out-off-plane compression.

The Fe oxide layer is thicker than that for Cr but both form stable protective layers for the metallic film. The roughness of the underlying metal layer also shows characteristic differences with Cr being rougher than Fe. Therefore, Cr buffer layers can be used to introduce additional roughness into epitaxial Fe/Cr superlattices to increase the giant magnetoresistance effect [13, 16].

The [Fe (4.8 Å)/Cr (13 Å)]$_{50}$ superlattice, discussed next, has a record GMR amplitude of 220% [13] which makes its structure particularly interesting. High-angle XRD shows that also Fe/Cr superlattices can be grown epitaxially on MgO(001) using MBE [13]. Thanks to the small lattice mismatch between Fe and Cr (0.6%) and their identical crystal structure (bcc) the layers grow coherently. In contrast to sputter deposition [17], epitaxial growth is observed (i) for any substrate temperature between 0 and 600 °C [16], (ii) for various deposition rates and (iii) independent of which material (Fe or Cr) is used for the starting layer. The SA XRD measured spectrum and its simulation (figure 2) show pronounced peaks being the first- and second-order superlattice Bragg peaks and fast oscillatory Kiessig

Table 1. Parameters used for the simulations of the XRD spectra shown in figures 1 and 2. σ_i are the rms roughness of the different interfaces.

	Fe	Cr	$[Fe/Cr]_{50}$
Oxide composition	Fe_3O_4	Cr_2O_3	mixed oxide
Oxide thickness (Å)	23.6	14.1	15
Fe thickness (Å)	276.8	—	4.8
Cr thickness (Å)	—	352.4	13.0
Cr buffer thickness (Å)	—	—	43
σ_{oxide} (Å)	3.5	2.7	6
σ_{Fe} (Å)	3.8	—	3
σ_{Cr} (Å)	—	10	3
$\sigma_{Cr\ buffer}$ (Å)	—	—	5
$\sigma_{substrate}$ (Å)	1.4	2.3	3.4

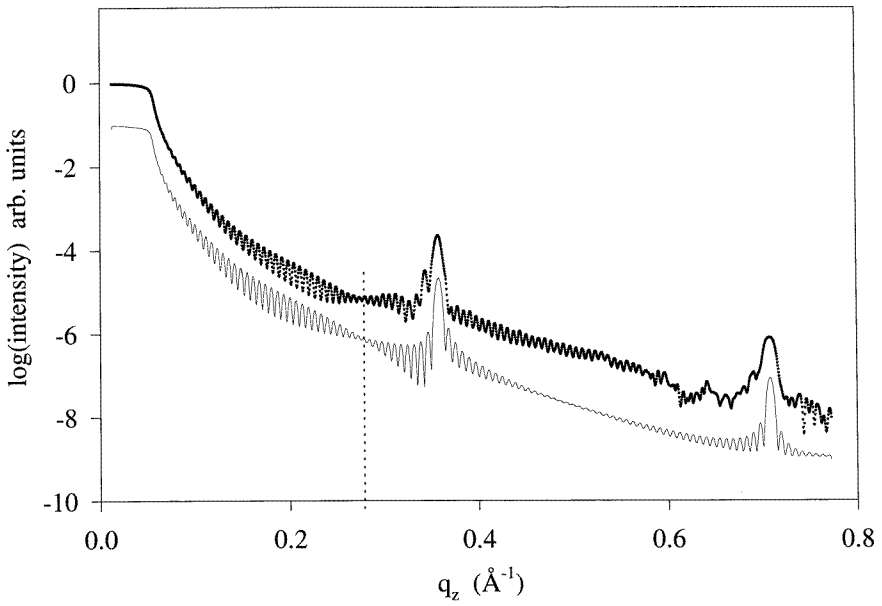

Figure 2. Specular XRD intensity as a function of the vertical scattering vector q_z. The measured spectrum (data points) and the simulation (thin line) of an [Fe (4.8 Å)/Cr (13 Å)]$_{50}$ superlattice are shown. The parameters of the simulations are summarized in table 1. The dashed line indicates the node in the Kiessig fringes which is also reproduced by the simulation. The spectra are offset for clarity.

fringes, again related to the total thickness of the film. The typical values for layer roughness and oxide properties (the superlattice had no protection layer) obtained from the analysis of the single layers had been used as input parameters for the simulation. The agreement between measurement and simulation is quite striking. Note that also details like the node in the Kiessig fringes at $q_z \approx 0.28$ Å^{-1} is well reproduced (dashed line in figure 2). This spectrum was measured with a x-ray wavelength off any absorption edge of either Fe or Cr. Accordingly, the material contrast between Fe and Cr is rather low because of their similar electron density. But obviously it is possible to simulate XRD

spectra of such low-contrast systems as Fe/Cr with high accuracy. This allows extraction of quantitative information about the interface structure, different form qualitative discussions of XRD spectra presented so far [6, 7, 18–20]. Furthermore, it should be noted that the spectrum shows very pronounced superlattice peaks [13, 21] although for this sample the interface roughness was intentionally increased to enhance the high GMR value. Often, XRD spectra of Fe/Cr superlattices reported in the literature show even less structure [18, 22, 23]. Smoother interfaces can be obtained by omitting the Cr buffer and growing the sample at elevated temperature [24, 25]. However, growth at elevated temperatures might cause some interdiffusion at the interfaces [26]. Offset θ–2θ SA XRD scans also show pronounced superlattice Bragg peaks indicating a high degree of vertical correlation of the interface roughness, i.e. that subsequent interfaces tend to replicate the structure of the previously grown ones.

4. Summary

We have presented a detailed, qualtitative structure analysis of an [Fe (4.8 Å)/Cr (13 Å)]$_{50}$ superlattice grown epitaxially on MgO(001). The analysis was done by simulation of the XRD spectrum using as input parameters the structural properties of the components obtained from independent measurements on single Fe and Cr films. The good quantitative agreement between measurement and simulation shows that even the structure of superlattices with a low contrasting their electron density can be determined using x-ray diffraction.

Acknowledgments

This work is financially supported by the Belgium Concerted Action (GOA) and Interuniversity Attraction Poles (IUAP) programs. RS was supported by the HCM Program of the EC. We would like to thank B Lengeler for the opportunity to use his diffractometer.

References

[1] Baibich M N, Broto J M, Fert A, Nguyen Van Dau F, Petroff F, Etienne P, Creuzet G, Friederich A and Chazelas J 1988 *Phys. Rev. Lett.* **61** 2472
[2] Verbanck G, Temst K, Mae K, Schad R, van Bael M J, Moshchalkov V V and Bruynseraede Y 1997 *Appl. Phys. Lett.* **70** 1477
[3] Hood R Q, Falicov L M and Penn D R 1994 *Phys. Rev.* B **49** 368
[4] Asano Y, Oguria A and Maekawa S 1993 *Phys. Rev.* B **48** 6192
[5] Barnas J and Bruynseraede Y 1996 *Phys. Rev.* B **53** 5449
[6] Fullerton E E, Kelly D M, Guimpel J, Schuller I K and Bruynseraede Y 1992 *Phys. Rev. Lett.* **68** 859
[7] Beliën P, Schad R, Potter C D, Verbanck G, Moshchalkov V V and Bruynseraede Y 1994 *Phys. Rev.* B **50** 9957
[8] Fullerton E E, Schuller I K, Vanderstraeten H and Bruynseraede Y 1992 *Phys. Rev.* B **45** 9292
[9] Sinha S K, Sirota E B, Garoff S and Stanley H B 1988 *Phys. Rev.* B **38** 2297
[10] Holý V, Kubeña J, Ohídal I, Lischka K and Poltz W 1993 *Phys. Rev.* B **47** 15 896
[11] Holý V and Baumbach T 1994 *Phys. Rev.* B **49** 10 668
[12] Schlomka J-P, Tolan M, Schwalowsky L, Seeck O H, Stettner J and Press W 1995 *Phys. Rev.* B **51** 2311
[13] Schad R, Potter C D, Beliën P, Verbanck G, Moshchalkov V V and Bruynseraede Y 1994 *Appl. Phys. Lett.* **64** 3500
[14] Sevenhans W, Locquet J-P and Bruynseraede Y 1986 *Rev. Sci. Instrum.* **57** 937
[15] Stierle A, Boedeker P and Zabel H 1995 *Surf. Sci.* **327** 9
[16] Schad R, Potter C D, Beliën P, Verbanck G, Dekoster G, Langouche G, Moshchalkov V V and Bruynseraede Y 1995 *J. Magn. Magn. Mater.* **148** 331

[17] Fullerton E E, Conover M J, Mattson J E, Sowers C H and Bader S D 1993 *Phys. Rev.* B **48** 15 755
[18] Matson J E, Brubaker M E, Sowers C H, Conover M, Qiu Z and Bader S D 1991*Phys. Rev.* B **44** 9378
[19] Colino J M, Schuller I K, Korenivski V and Rao K V 1996 *Phys. Rev.* B **54** 13 030
[20] Colino J M, Schuller I K, Schad R, Potter C D, P Beliën, Verbanck G, Moshchalkov V V and Bruynseraede Y 1996 *Phys. Rev.* B **53** 766
[21] The second-order superlattice Bragg peak is at $2\theta = 11.5^\circ$ when measured with Cu Kα wavelength.
[22] Joo S, Obi Y, Takanashi K and Fujimori H 1992 *J. Magn. Magn. Mater.* **104** 1753
[23] Chen L H, Tiefel T H, Jin S, Van Dover R B, Gyorgy E M and Fleming R M 1993 *Appl. Phys. Lett.* **63** 1279
[24] Wolf J A, Leng Q, Screiber R, Grünberg P A and Zinn W 1993 *J. Magn. Magn. Mater.* **121** 253
[25] Potter C D, Schad R, Beliën P, Verbanck G, Moshchalkov V V, Bruynseraede Y, Schäfer M, Schäfer R and Grünberg P 1994 *Phys. Rev.* B **49** 16 055
Schad R, Potter C D, Beliën P, Verbanck G, Moshchalkov V V, Bruynseraede Y, Schäfer M, Schäfer R and Grünberg P 1994 *J. Appl. Phys.* **76** 6604
[26] Davies A, Stroscio J A, Pierce D T and Celotta R J 1996 *Phys. Rev. Lett.* **76** 4175